Obtaining K and D meson properties from lattice QCD

Oscar Simpson
Supervisor: Dr. B. Chakraborty

May 2021

Abstract

Quantum Chromodynamics (QCD) is an integral component of the Standard Model (SM). At low energies QCD cannot be solved perturbatively, however it is possible to find solutions by coarse-graining and computing on a lattice. Throughout, a Highly Improved Stagged Quark (HISQ) action is used. From statistical ensembles of 2-point correlators we are able to extract properties of particles such as the mass and partial decay width of mesons, using the well-known `corrfitter` and `lsqfit` Python packages[**lepage2020lsqfit**, 1]. These properties depend both with a lattice discretisation error, and with the (unphysical) light quark mass of the HISQ action. Extrapolation to the chiral/contiuum limit is also performed in order to obtain properties that are physical. In particular, these techniques are well suited to work with stranged and charmed mesons on a $N_f = 2 + 1 + 1$ quark sea. The mass of mesons calculated here $TODO$ is consistent with results in literature.

Contents

1 Introduction

1.1 Standard Model

The Standard Model is currently the most accurate model of particle physics. It describes fermions: quarks (q), leptons (l), and their antiparticles, denoted with an overline ($\overline{q}$). It also describes the gauge bosons which mediate the strong, weak, and electromagnetic (EM) fields.

There are 6 flavours of quarks, in 3 different generations. Quarks are coupled to the strong, weak, and EM interactions. The leptons, also in 3 generations, are coupled to the EM field if they are charged, and to the weak force. This project is to study the spectra of bottomonium mesons. These are hadrons composed of a bottom quark and any antiquark (or an antiparticle of this). The weak and EM interactions are completely neglected, leaving only the strong interaction which is governed by the theory of Quantum Chromodynamics (QCD).

1.2 Quantum Chromodynamics

QCD is a $SU(3)$ gauge field theory governing the interactions of quarks and gluons. As quarks are fermions, they are described by a Dirac lagrangian coupled to an external gauge field. For a quark field annihilation operator ψ_f, Dirac field creation operator $\overline{\psi} = \psi_f^\dagger \gamma^0$ with quark flavour f, we have[2, 3]:

$$\mathcal{L} = \sum_f \psi_f^\dagger (i \not{D} - m_f) \psi_f - \frac{1}{4} F^a_{\mu\nu} F_a^{\mu\nu} \tag{1}$$

In this Lagrangian we have a gauge covariant derivative $\not{D} = \not{\partial} + i g_s \not{A}^a \lambda_a / 2$. Here and in the rest of this section, we leave the indices referring to colour implicit. However to be clear, the quarks carry a conserved *colour charge* analogous to the electric charge in QED. There are three separate *colours* which are often called *red*, *green*, and *blue*[1]. The colour of a quark is represented by a colour spinor, which is the space acted on by the λ_a. It is these indices, referring to the matrix multiplication, that are omitted.

The other important quantity is the gluon field strength tensor:

$$F^a_{\mu\nu} = \partial_\mu A^a_\nu - \partial_\nu A^a_\mu - g_s f_{abc} A^b_\mu A^c_\nu \tag{2}$$

Here the latin indices label the 8 generators[2] ($t_a = \lambda_a/2$) of the QCD $\mathfrak{su}(3)$ Lie algebra with (totally antisymmetric) structure constants $[t_a, t_c] = i f_{abc} t_c$. These generators are considered to be linearly independent colour charges of gluons. A^a_μ are the respective 4-potentials, which are coupled to the quarks.

Unlike in QED, QCD allows for self-interaction of the gauge bosons. As a result, QCD is known as an asymptotically-free theory: as interactions are taken to higher energies, the forces involved become weaker. This leads to colour confinement, where only bound states with zero overall colour charge can be isolated. Traditional perturbation theory

[1] Although, the choice of basis is arbitrary and can be transformed by any matrix $U \in SU(3)$.

[2] λ_a are the Gell-Mann matrices, which form a basis of $SU(3)$.

expands a system at low energy, but in the case of QCD this would give divergent forces which would invalidate such a method. Instead, a common approach is solving systems on a lattice.

1.3 Lattice QCD

Lattice QCD is a method to solve QCD systems by placing the fields on a spacetime lattice. To see how this is done we first consider the path integral formulation of QFT. To compute the expectation of an operator, we take a functional integral of the Lagrangian over all possible field configurations[4, 3]

$$\langle \mathcal{O} \rangle = \frac{1}{\mathcal{Z}} \int \mathcal{D}\psi \, \mathcal{O} \exp\left(i \int \mathrm{d}^4 x \, \mathcal{L}(\psi, \partial\psi) \right), \tag{3}$$

$$\mathcal{Z} = \int \mathcal{D}\psi \quad \exp\left(i \int \mathrm{d}^4 x \, \mathcal{L}(\psi, \partial\psi) \right), \tag{4}$$

where $\mathcal{Z}$ is the partition function. This is named in analogy with the statistical partition function, which can be obtained by performing a Wick rotation $t \mapsto it$.

Clearly it is not usually feasible to integrate over an infinite-dimensional space of functions, so we use a technique called regularisation. To do this we replace the $4D$ continuum integral by a spacetime lattice. Often an isotropic lattice is chosen (with lattice spacing a), however the main aim of this project is to use an anisotropic lattice the spatial and temporal lattice spacings differ.

We define the quark fields[3] $\psi(x)$ only on lattice points x_μ, and the gluon fields $U_{\hat{\delta}}(x) = U(x, x + \hat{\delta})$ defined on the links between the lattice points. The links are specified as written, by a point x^μ and a unit vector $\hat{\delta}^\mu$ specifying the direction along the lattice. The conjugate field $U^\dagger_{\hat{\delta}}(x) = U(x + \hat{\delta}, x)$ gives the link from $x + \hat{\delta}$ back to x. Once we have our particle fields, it is possible to replace derivatives with differences in fields at adjacent lattice sites. One can then construct an appropriate gauge invariant action, called the Wilson action.

We hope that by using this lattice model of QCD, we can produce sensible results in the limit of a short lattice spacing. Unfortunately, when the computations are carried out there are a lot of discretisation errors[5]. By a careful choice of discrete derivative, we can remove $\mathcal{O}(a)$ error terms. The $\mathcal{O}(a^2)$ error terms can also be removed by adding and subtracting appropriate counterterms[6]. This leaves us with a discretised theory with errors in $\mathcal{O}(a^3)$, which we hope is small enough that our extrapolation to $a \to 0$ is accurate.

1.4 HISQ Action

$$M^{-1} = \frac{-i\gamma_\mu \sin(ap_\mu)/a + m}{\sum_{\mu=0}^{3} \sin^2(ap_\mu)/a^2 + m^2} \tag{5}$$

TODO: this

1.5 Correlators

TODO: this, including moving 2-pt correlator eq from prelimn to here

1.6 Relating Lattice and Physical

TODO: This is for chiral-continuum limit etc. Any mass specified in lattice units can be converted into physical units by $m = (\hbar c) m^{\text{lattice}}/a$.

2 Statistical Methods and Data

2.1 Jacknife Averaging

Given a large sample of data with completely unknown errors, we often want to compute unbiased estimators for statistical parameters. One such way is to use Jacknife averaging[7]. Consider a sample of n i.i.d. values $x_i \sim F$. Construct n mean estimates $\overline{x}_i = \sum_{j \neq i} \frac{x_j}{n-1}$. The average of these sample means $\overline{x} = \sum_i \frac{\overline{x}_i}{n}$ is precisely the mean of the whole sample, and the error on this estimate is given by the variance $\text{Var}[\overline{x}] = \frac{n-1}{n} \sum_i (\overline{x}_i - \overline{x})^2$ of the distribution of $\overline{x}_i$. That is, we have an unbiased estimator for the mean and standard defiation of F given by $\overline{x} \pm \sqrt{\text{Var}[\overline{x}]}$. In fact by replacing the means $\overline{x}_i$ above by (almost) any estimator $\overline{\theta}_i$, it is possible to construct an new estimator, using a slightly more laborious method, which has an asymptotically smaller bias[8].

2.2 χ^2 Fitting

2.3 Bayesian Analysis

Using the `corrfitter`[1] Python package, it is possible to perform a least-squares regression on our 2-point correlator data. For a given set of priors and a data set, the least-squares regression gives best-fit values for parameters of choice. In the context of this project, we are interested in fitting the amplitudes a_n, a_{on} and the log of the energy differences, $\log(\text{d}E_n)$, $\log(\text{d}E_{on})$. In particular, the log of energy differences allows us to implicitly force the energy levels of the fit to strictly increase.

For a fit of this type, we expect a good quality fit to have $\chi^2/\text{dof} \approx 1$. Values much larger than this are a poor fit, and values closer to 0 could indicate overfitting. There are other measures of goodness-of-fit such as the Gaussian Bayes Factor and the Q value, however their use is unnecessary here and we will continue only using the χ^2 measure.

2.4 Data

Data for this whole project has been provided by Dr. B. Chakraborty. This data has been produced by using relativistic HISQ action for both valuence and sea quarks on publicly available gauge configurations generated by MILC collaboration given in Table 1. The configurations have sea quark effects from up/down (light), strange, and charm quarks.

Label	a (fm)	$N_t \times N_x^3$	m_l/m_s	$n_{\text{cfg}} \times n_{\text{c}}$	β	w_0/a	$am_l^{\text{sea/val}}$	am_s^{sea}	am_c^{sea}	am_s^{val}	am_c^{val}	Z_{disc}
Very Coarse	0.1509	48×32^3	0.036	998×16	5.8	1.1367(5)	0.002 35	0.0647	0.831	0.0678	0.8605	0.991 97
Coarse	0.124 04	64×24^3	0.2	1053×16	6.0	1.3826(11)	0.0102	0.0509	0.635	0.0656	0.664	0.996 83
Fine	0.090 23	96×32^3	0.2	499×16	6.3	1.9006(20)	0.0074	0.037	0.440	0.0376	0.449	0.998 92

Table 1: Parameters of the data used in the main part of this project. Corresponding to sets 1, 5, 6 from table I[9] respectively. TODO: update caption

By using a finite lattice we have discretisation errors (discussed in Section 1.3), which we can only eliminate by extrapolating from multiple datasets, to the contiuum limit. Additionally, for computational reasons it is not possible to use physical light quark masses for all lattice sizes. As a result, we must also extrapolate to the chiral limit, where $m_l = 0$, which is close to the physical value of $m_l \approx 0.02 m_s$.

TODO: Describe how project has evolved into a data analysis project.

3 Preliminary study

Using Jacknife averaging, an existing dataset[10] was analysed. This is a set of 2-point correlators for a $D-$meson ($c\overline{q}$). In this dataset there are $n = 489$ gauge configurations, with $T = 96$ time slices. The average over Jacknife averages is shown in Figure 1. From[11] we know that these correlators are expected to follow the following relationship,

$$G(t) = \sum_n a_n^2 (e^{-E_n t} + e^{-E_n (T-t)}) + (-1)^t \sum_n a_{on}^2 (e^{-E_{on} t} + e^{-E_{on} (T-t)}), \tag{6}$$

where E_n gives the energy of the n^{th} excited state, and a_n gives its amplitude. In this expression, the reflected $T-t$ terms are due to the periodic boundary conditions, and the E_{on} terms are oscillatory contributions due to the opposite parity state in the staggered quark analysis.

TODO: Switch to the new datafile for this section

If we assume the oscillatory terms are small then one can look near the middle of the data (shown in Figure 1). Here the only relevant term is the ground state (a_0, E_0). As a result, in this region we should be able to compute an estimate for the ground state effective mass,

$$m_{\text{eff}}(t) = \log\left(\frac{G(t)}{G(t+1)}\right). \tag{7}$$

When actually computing this value, we must make sure that we do not go past halfway through the data, as the second half (with rising exponentials) will lead to a negative effective mass with the same magnitude. As shown in Figure 2, for the provided (non-Gold D meson on a fine lattice), the effective mass is approximately $m_{\text{eff}} \approx 0.87 \approx 1900\,\text{MeV}$. To compute this value we took the average of the time-dependent values for time steps $t = 24 - 36$, where the data has clearly plateaued but still has small errors.

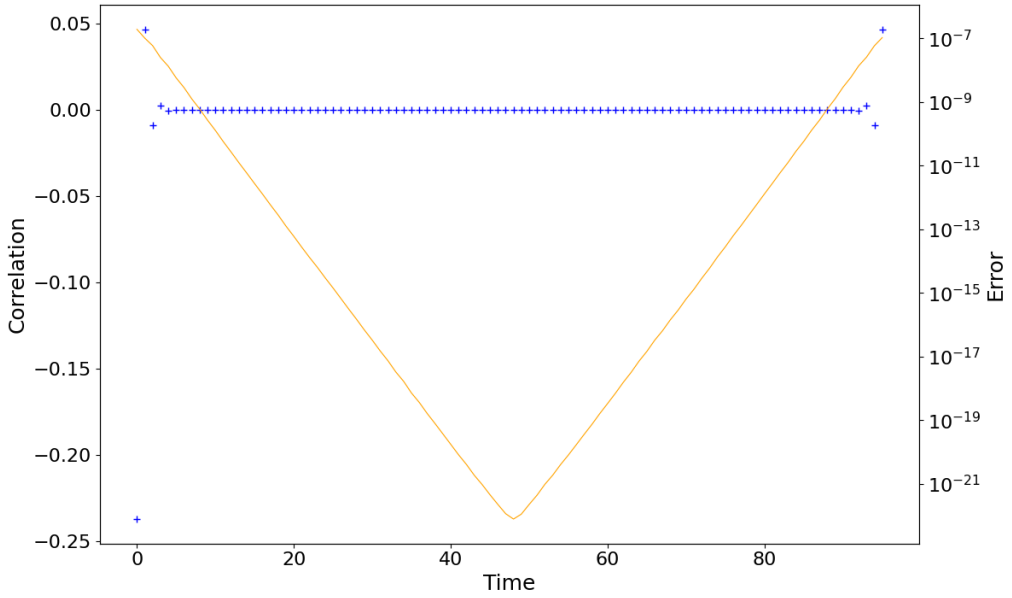

Figure 1: Average 2 point correlator for $n = 489$ gauge configurations on a fine lattice. Computed by using Jacknife averaging. Away from the endpoints correlator values are very small, which is consistent with our assumption that our exponentials decay sufficiently quickly.

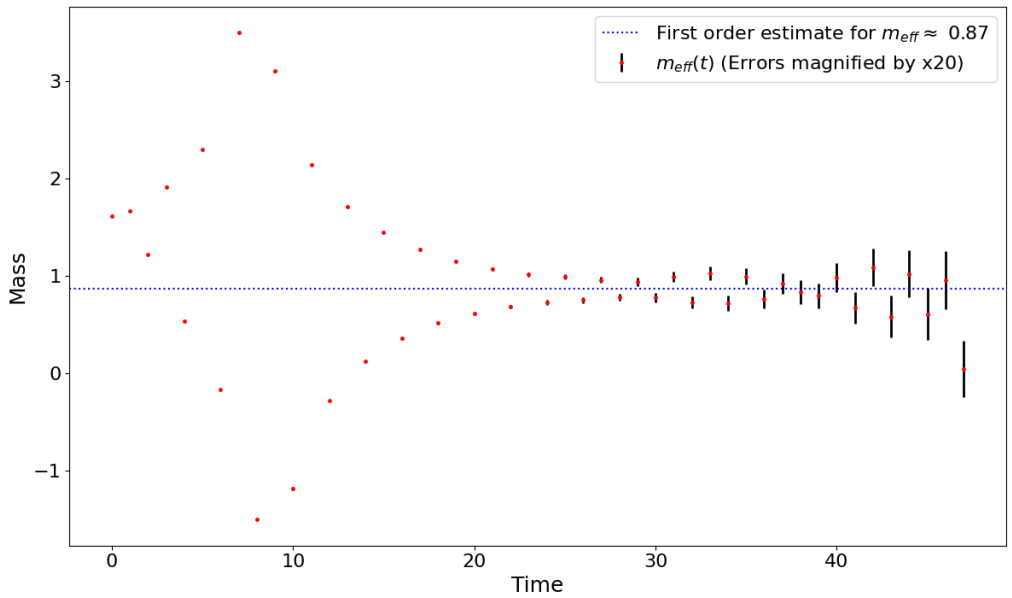

Figure 2: Estimate for m_{eff} using Equation 7.

4 Data Analysis

Throughout this section, all correlator data has been Jackknife averaged to give an estimated Gaussian variable at each time slice. The analysis code is a very heavily modified version of code again provided by Chakraborty, which includes optimised prior values. Throughout this analysis we are fitting up to 6 terms in the correlator (Equation 6). It is not reasonable to extract physical results from most of these terms, however we can certainly look at the ground state of each meson. Taking the most reliable value of meson mass for each of the data sets, it is possible to extrapolate to the chiral and contiuum limits to compute final estimates for the neutral K and D meson masses.

During the analysis, there are two main fitting parameters that are varied. t_{min} tells the fitting software how many time slices to ignore from the start and the end of each set of correlator data. This is useful as there are extra effects happening at these early time scales, and we would like to ignore these for simplicity. The other parameter, n, corresponds to the number of exponentials for which we are providing prior data. Studying energy levels larger than n is completely unreasonable as these are only used to acheive a better fit, and the values are unphysical.

For all datasets that are analysed, we limit the fitting for K mesons to only have $t_{\text{min}} = 3$. For D mesons we vary this as $t_{\text{min}} \in \{3, 4, 5, 6, 7, 9\}$. For both mesons, we also vary $n \in \{1, \ldots, 6\}$. In all of the following plots, $n = 4$ was determined to be the most reliable point, so all values given on the plots are evaluated here. For plots showing fitting results, error bars are indicated in red. When a data point (error bar) appears missing it is either too large (small) to be shown on the scale. For convenience, the first 4 data points of the fitting quality plots have also been reproduced on the plots, as the majority of these points are far too large to be shown on the same scale as the rest of the points.

4.1 Fit convergence

The fine dataset corresponds to a lattice spacing $a \approx 0.09\,\text{fm}$ and a light quark mass $m_l \approx 0.2m_s$. For the K meson, it is clear that for any value of $n \geq 4$, the fit has converged (Figure 3[3]). Inspection of the results for D meson show that the fits tend to converge first for $n = 3$ or 4. Now we turn to the fit quality, where as we can see in Figure 4, the fitting converged well for all t_{min} and for all $n \geq 4$.

The coarse dataset corresponds to a lattice spacing $a \approx 0.12\,\text{fm}$ and a light quark mass $m_l \approx 0.2m_s$. In this dataset, we can see that the K meson values (Figure 5) actually converge for $n = 3$. More generally, the fit quality (Figure 6) suggests that $n = 3$ or 4 are the earliest parameters that converge, although this is more reliable for higher t_{min}.

The very coarse dataset corresponds to a lattice spacing $a \approx 0.15\,\text{fm}$ and a light quark mass $m_l \approx 0.036m_s$. Here we see that the K meson fit (Figure 7) apepars to converge even for $n = 2$. The fit quality plots (Figure 8) show a different result however. Even at higher t_{min}, the χ^2 parameter does not reach a reasonable value until at least $n = 3$.

[3]Plots of this form have been produced for all combinations of dataset and t_{min}, however where they do not add to the discussion, they have been ommitted.

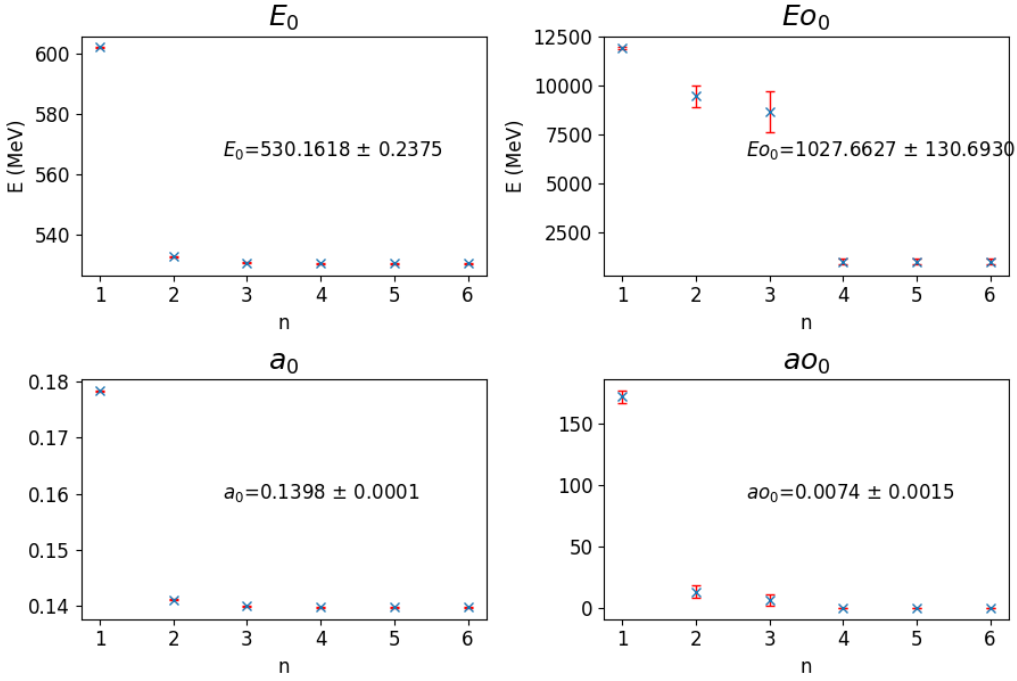

Figure 3: K meson fitting results on a fine lattice.

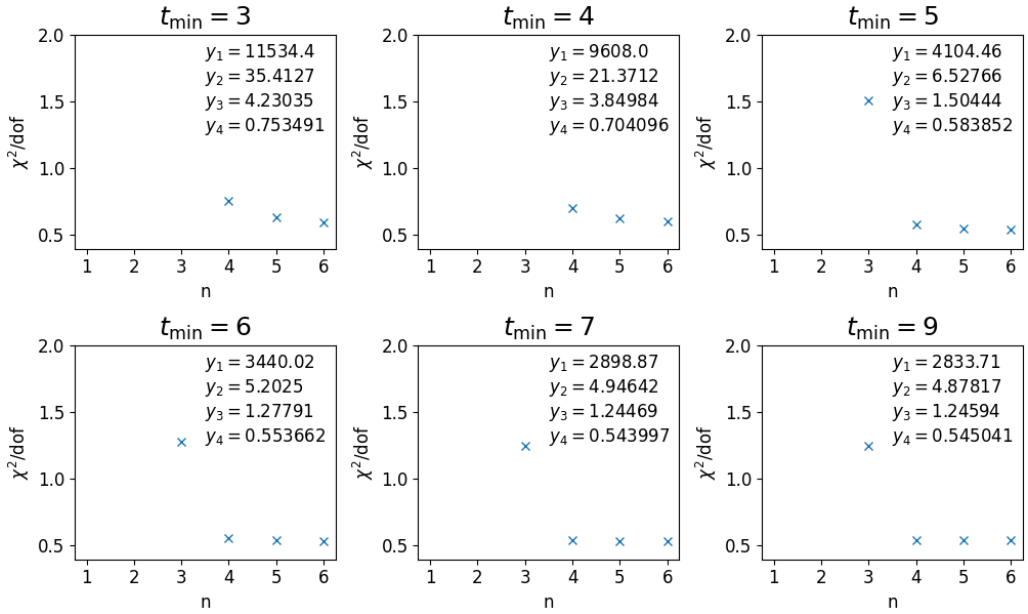

Figure 4: Fitting quality for fine lattice.

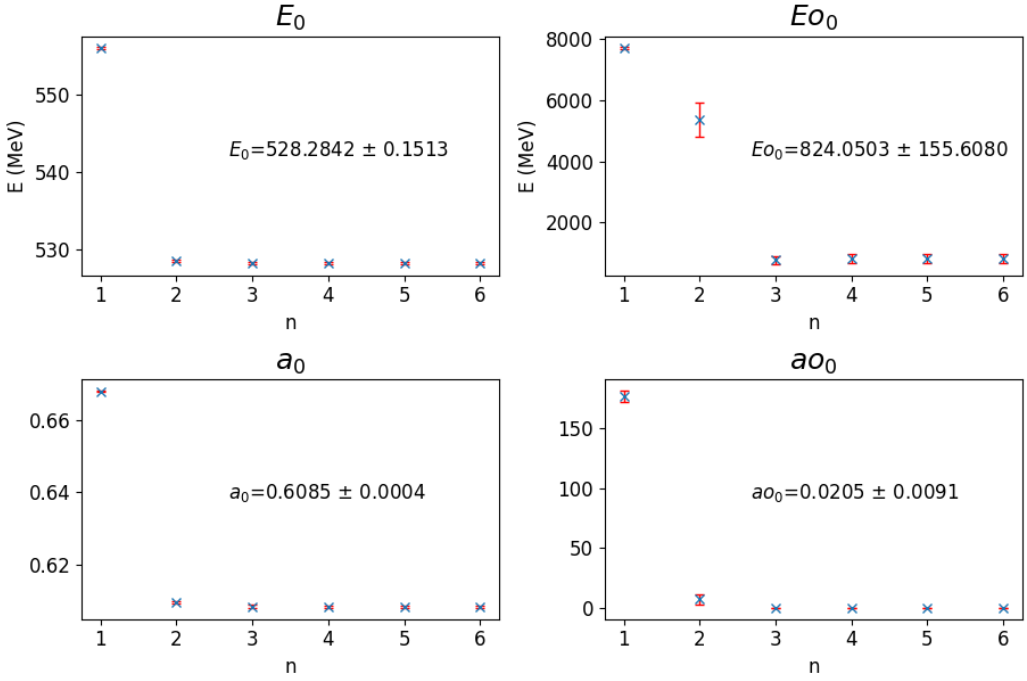

Figure 5: K meson fitting results on a coarse lattice.

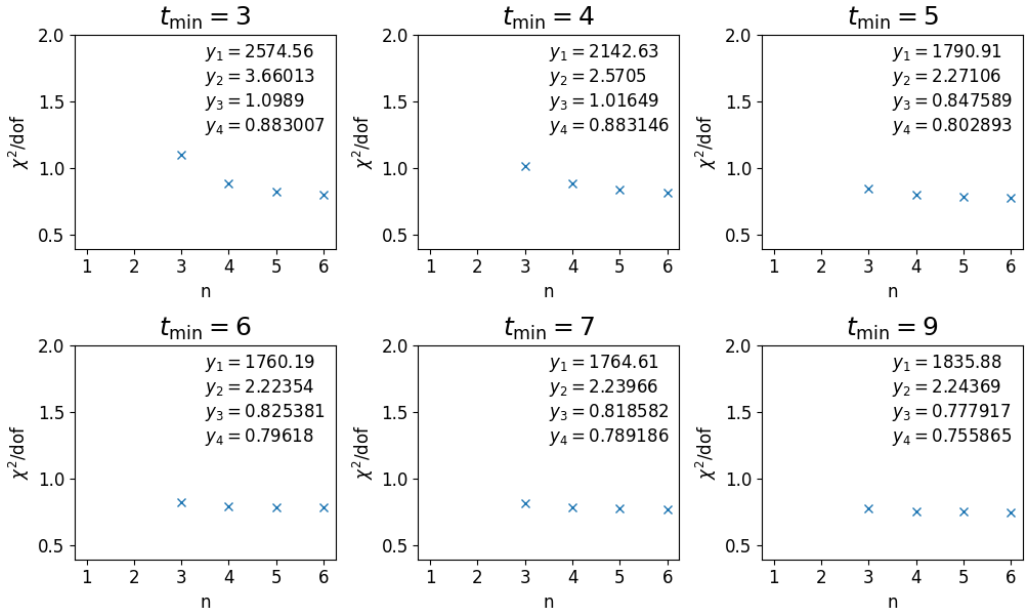

Figure 6: Fitting quality for coarse lattice.

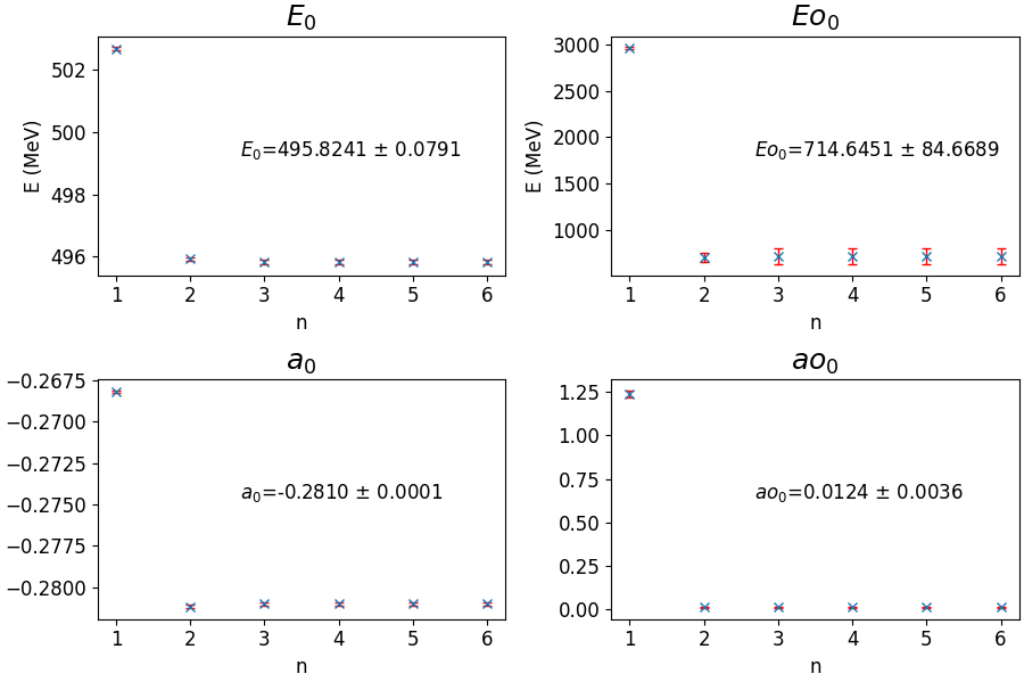

Figure 7: K meson fitting results on a very coarse lattice.

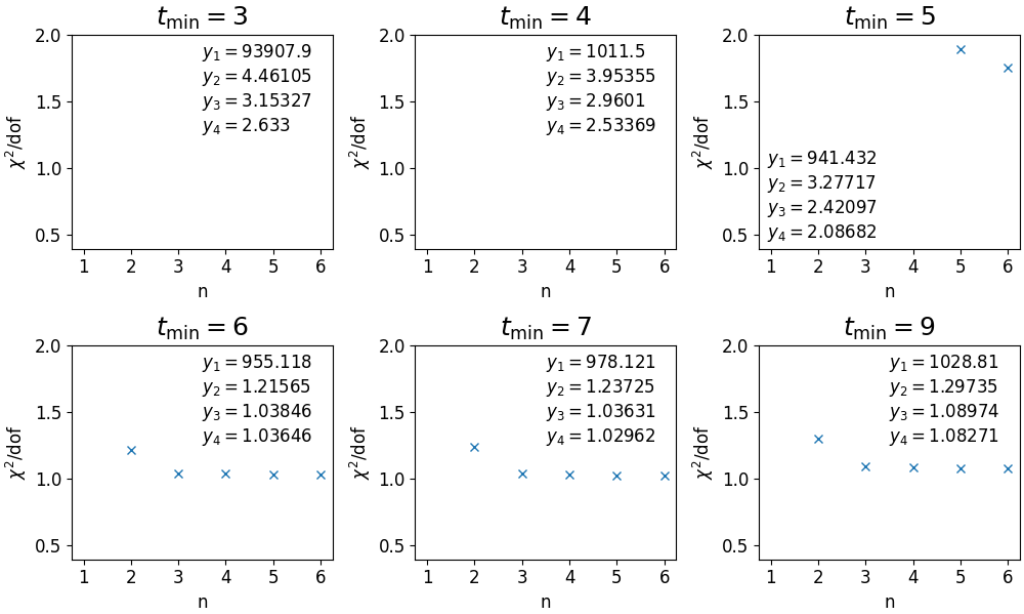

Figure 8: Fitting quality for very coarse lattice.

			E_0 (MeV)		$\lvert a_0\rvert$	
Label	a (fm)	m_l/m_s	K	D	K	D
Very Coarse	0.15	0.036	495.92(08)	1887.3(51)	0.281 01(11)	0.2286(65)
Coarse	0.12	0.2	528.28(15)	1893.0(15)	0.608 53(37)	0.1880(12)
Fine	0.09	0.2	530.16(24)	1889.3(11)	0.139 78(12)	0.1242(07)

Table 2: Results from fitting all datasets. $t_{\min} = 6$ for D mesons, and $n = 4$ for all results. Uncertainties given in parentheses are statistical.

4.2 Results

Taking into account the values of parameters for which all the datasets had reliable fits, the smallest (and least likely to lead to overfitting) viable choices for the parameters are $n = 4$ and $t_{\min} = 6$. The collection of E_0 and a_0 values that are found with these parameters is given in Table 2. The energy values here seem reasonable as they correspond roughly to the masses provided in [12]: $m_K \approx 498\,\text{MeV}$ and $m_D \approx 1865\,\text{MeV}$. Of course, these values are far outside the provided statistical error bounds, but this is expected as we have both unphysical quark masses, and discretisation errors. Our next step will extrapolate our values to the chiral-continuum limit, which should give accurate results.

5 Chiral-Continuum Extrapolation

Using the results we found above, it should be possible to extrapolate down to the chiral (physical light quark mass) and continuum (to avoid discretisation errors) limits. From Equation 16 in [13] we know that we should be able to model this extrapolation well. However, we have a total of 6 values that we are fitting, so it would be dubious to fit a model with any more than 6 parameters. As a result, we take the 3 lowest order terms (each produces a pair of parameters for K and D mesons respectively) which gives us

$$m = m_{\text{phys}}\Big(1 + c_\delta \frac{m_l}{m_s}\Big)\Big(1 + c_{a^2} a^2\Big). \tag{8}$$

When we perform a χ^2 fit to these values[4] we find a $\chi^2/\text{dof} = 0.23$ which signifies a good quality fit. This also does not appear to be overfit, which was a concern given that we are fitting 6 parameters to 6 data points. Table 3 shows that the predicted values match very well with the observed values, as expected. Also shown are the extrapolated values which are consistent with results from the literature[12], $m_{K^0} = 497.611(13)\,\text{MeV}$ and $m_{D^0} = 1864.83(5)\,\text{MeV}$ to within 3σ of our statistical uncertainty.

TODO: Partial decay widths

[4]The priors used for this fit are drawn from the same source.

	E_0 (MeV)		Predicted E_0 (MeV)	
Label	K	D	K	D
Very Coarse	495.92(08)	1887.3(51)	495.92(08)	1887.3(51)
Coarse	528.28(15)	1893.0(15)	528.31(25)	1892.8(15)
Fine	530.16(24)	1889.3(11)	530.13(24)	1889.4(11)
Chiral/Continuum limit	-	-	494.5(11)	1874.6(88)

Table 3: Comparison of observed and predicted mass values, including the extrapolated chiral/continuum limit values.

6 Conclusion

6.1 Results

This project has been primarily focussed on data analysis. The first part was important as a first step to check that data was in fact of the form that we expected. Indeed we found that for a specific set of HISQ parameters, $m_{D^0}^{\text{eff}} \approx 1900\,\text{MeV}$. This approximation only involved fitting the first (i.e. ground state) exponential and no oscillatory terms, but still gave a result within around 5 % of what was expected.

The second part constituted the majority of the effort of the project. Here, 3 datasets with varying light quark mass and lattice spacing were analysed using an existing tool. This gave far more precise values for both the mass and amplitudes of the mesons, presented in Table 2. Again we saw that the meson masses were consistent with expected results, except with this data we were also able to notice the variation with respect to the HISQ parameters.

Finally, with a selection of meson masses, it was possible to extrapolate to the chiral/continuum limit. The aim here was to find physical meson masses and partial decay widths. Table 3 shows the extrapolated masses, which were within 3σ of the literature values. TODO: Partial decay widths

6.2 Further Work

This project followed existing techniques in lattice NRQCD so the next steps have already been explored well. The key advances to make would likely include adding more datasets. That is, a larger variety of light quark masses, and lattice spacings. By increasing the number of datasets analysed it would become viable to fit more parameters to Equation 8. This could give a tighter fit and thus reduce the statistical error on the final results. With careful enough analysis it is possible to also calculate masses, amplitudes, and decay widths for excited states. This expansion in scope can be seen as a subset of the analysis performed in [9].

Alternatively, similar analysis could be carried out on heavier mesons e.g. $b\bar{b}$ bottomonium mesons, such as that carried out in [14]. TODO: Slightly expand further work?

References

[1] G Peter Lepage. *corrfitter*. Version 8.1.1. 2020. URL: https://github.com/gplepage/corrfitter.

[2] G. Shaw F. Mandl. *Quantum Field Theory*. John Wiley & Sons, 2010.

[3] Brian Colquhoun. "Bottomonium and B Physics with Lattice NRQCD b Quarks". University of Glasgow, 2015.

[4] R. P. Feynman. "Space-Time Approach to Non-Relativistic Quantum Mechanics". In: *Rev. Mod. Phys.* 20 (2 Apr. 1948), pp. 367–387. DOI: 10.1103/RevModPhys.20.367.

[5] Christof Gattringer and Christian B Lang. *Quantum Chromodynamics on the Lattice: An Introductory Presentation*. eng. Vol. 788. Lecture notes in physics. Berlin, Heidelberg: Springer Berlin / Heidelberg, 2009. ISBN: 3642018491.

[6] K. Symanzik. "Continuum limit and improved action in lattice theories: (I). Principles and ϕ^4 theory". In: *Nuclear Physics B* 226.1 (1983), pp. 187–204. ISSN: 0550-3213. DOI: https://doi.org/10.1016/0550-3213(83)90468-6.

[7] Bradley Efron. *The jackknife, the bootstrap and other resampling plans*. SIAM, 1982.

[8] Avery McIntosh. "The Jackknife estimation method". In: *arXiv preprint arXiv:1606.00497* (2016).

[9] Bipasha Chakraborty et al. "Improved V_{cs} determination using precise lattice QCD form factors for $D \to Kl\nu$". In: *arXiv e-prints* (2021), arXiv–2104.

[10] TBC. 2pt_hisq_msml5_fine_D_nongold_489conf.dat. 2020.

[11] Bipasha Chakraborty. "Precision tests of the standard model using lattice QCD". University of Glasgow, 2016.

[12] Particle Data Group et al. "Review of Particle Physics". In: *Progress of Theoretical and Experimental Physics* 2020.8 (Aug. 2020). 083C01. ISSN: 2050-3911. DOI: 10.1093/ptep/ptaa104. eprint: https://academic.oup.com/ptep/article-pdf/2020/8/083C01/34673740/rpp2020-vol2-2015-2092_18.pdf. URL: https://doi.org/10.1093/ptep/ptaa104.

[13] Bipasha Chakraborty et al. "Nonperturbative comparison of clover and HISQ quarks in lattice QCD and the properties of the phi meson". In: *arXiv preprint arXiv:1703.05552* (2017).

[14] WG Parrott et al. "Towards accurate form factors for B to light meson decay from Lattice QCD". In: *arXiv preprint arXiv:2010.07980* (2020).